ELSEVIER

Calculation of Oxygen Pressures in Tissue with Anisotropic Capillary Orientation. I. Two-Dimensional Analytical Solution for Arbitrary Capillary Characteristics

LOUIS HOOFD

Department of Physiology, Faculty of Medical Sciences, University of Nijmegen, Geert Grooteplein Noord 21, 6525 EZ Nijmegen, The Netherlands

Received 30 March 1993; revised 19 July 1994

ABSTRACT

In tissue with a distinct orientation of the oxygen supplying structures, the capillaries, a mathematical description of oxygen transport is feasible in terms of two-dimensional diffusion in a plane perpendicular to the capillaries. Muscle tissue is an example of a highly anisotropic tissue. With some additional simplifying assumptions, a solution can be constructed in terms of capillary sources for arbitrary capillary characteristics, in particular, capillary locations. The solution includes facilitated diffusion by myoglobin in the tissue. For homogeneous tissue, the solution becomes explicit allowing direct calculation of tissue oxygen pressure at any location in a field of simple geometry (circular, rectangular). Also, the size of the area into which each capillary distributes its oxygen, the oxygen supply area, is readily calculated.

1. INTRODUCTION

Calculation of oxygen pressures in tissue is a very complicated task in spite of the fact that the oxygen distribution process itself is quite simple [6, 20]. Oxygen-rich blood is supplied by the arterioles, branching into a capillary network draining into collecting venules. In this pathway, and particularly in the capillaries, oxygen is released and transported by diffusion. In the erythrocyte, the oxygen source, O_2 has to be released from its carrier the hemoglobin (Hb) to which it is reversibly bound. Many accompanying processes may be considered, e.g., CO_2 interaction with $Hb—O_2$ binding. Then, O_2 diffusion has to be considered through the erythrocyte, the blood plasma, the capillary wall and several tissue fractions. Reversible binding to myoglobin (Mb) occurs in red muscle tissue. Even when modeling simplified situations, a representative tissue system is much too complicated for purely numerical

MATHEMATICAL BIOSCIENCES 129:1–23 (1995)

655 Avenue of the Americas, New York, NY 10010
0025-5564/95/$9.50
SSDI 0025-5564(94)00049-6

computation (grid spacing < 1 μm, tissue dimensions ~ 100 μm and mixed boundary values coupled to the capillary flow pattern). Therefore, theoretical and computational development has concentrated on a special but important tissue, muscle tissue, where capillaries can be considered to run substantially in parallel. Then a distinct orientation can be discerned and the system can be handled separated into a z-direction along and an x, y-plane perpendicular to the orientation of the capillaries.

Even so, computation is a formidable task only feasible for simplified cases. The readiest simplification is to neglect diffusional effects in the z-direction, reducing the problem to a two-dimensional one. This seems appropriate since characteristic distances in the x, y-plane are of order 10^1 μm (capillary spacing) whereas in the z-direction this order is of 10^3 μm (capillary length). Indeed, the first modeling approach [16] was a solution for circular areas perpendicular to a centrally located capillary (Krogh cylinder). Later [13], the extension was made toward the third dimension by coupling planes in the z-direction through their successive capillary pO_2s.

The circular Krogh layout is much too simple to describe realistic muscle tissue [24, 25], but it can be generalized into a description for arbitrary capillary locations in a flat plane; first attempts were by [1, 11, 12]. In the present paper, the mathematical formulations and postulates and possibilities are investigated. The Krogh circle with one capillary source is extended to arbitrary shapes with several sources located arbitrarily. Facilitated diffusion by myoglobin is incorporated. The boundary conditions are reformulated correspondingly.

2. THEORY

2.1. *BASIC EQUATIONS*

The starting point for the theoretical treatment is the description of the diffusional transport of a species X in a nonmoving system of homogeneous diffusional properties by its flux $\vec{J}_X$:

$$\vec{J}_X = -D_X \vec{\nabla} c_X, \tag{2.1}$$

where D is diffusion coefficient and c concentration. This is an approximate description for low species concentrations and is considered to be valid for the species of interest, being oxygen and oxymyoglobin (O_2Mb).

Both carry one oxygen molecule so that the total flux of oxygen $\vec{J}$ is the sum of the two:

$$\vec{J} = \vec{J}\mathrm{O}_2 + \vec{J}\mathrm{O}_2\mathrm{Mb}.$$

(The particular species O_2, Mb, and $\mathrm{O}_2\mathrm{Mb}$ are not written as subscripts, but are added directly after the symbol, conforming to recent notational guidelines [17]). J can be expressed in terms of oxygen partial pressure p and myoglobin saturation s using (2.1) and Henry's law, $c\mathrm{O}_2 = \alpha\mathrm{O}_2 p$ where $\alpha\mathrm{O}_2$ is oxygen solubility:

$$\vec{J} = -\mathscr{P}\vec{\nabla}p^* \tag{2.2}$$

$$p^* = p + p_{\mathrm{F}}s, \tag{2.3}$$

where $\mathscr{P} = (D\mathrm{O}_2)(\alpha\mathrm{O}_2)$ is the oxygen permeability constant of the tissue and $p_{\mathrm{F}} = (D\mathrm{O}_2\mathrm{Mb})(c_{\mathrm{t}}\mathrm{Mb})/\mathscr{P}$ is called facilitation pressure [6]; p_{F} is a constant when total myoglobin concentration $c_{\mathrm{t}}\mathrm{Mb}$ is constant. Equations (2.2), (2.3) offer a most convenient way of incorporating Mb-facilitated O_2 diffusion. Without Mb, $p_{\mathrm{F}} = 0$ so that $p^* = p$ and plain, nonfacilitated O_2 diffusion is described. Incorporating Mb only involves replacing the oxygen pressure p by an oxygen driving force p^*. In addition, the local relationship between p and s must be known. This problem is extensively handled in the literature [5, 7, 15, 21]. For most of the tissue, chemical equilibrium can be assumed between Mb and O_2. Only near interfaces that the myoglobin cannot pass, such as cell boundaries, are deviations expected. This does not affect the validity of (2.2), (2.3), but now the relation between p and s will deviate from equilibrium. For tissue modeled as homogeneous, these deviations will occur at the capillary-tissue interface.

Finally, there is a mass balance between transport and chemical reaction of O_2. For O_2 transport we apply (2.2) and the net chemical reaction is expressed in terms of the consumption rate Q of the tissue (amount per unit time):

$$\mathscr{P}\nabla^2 p^* = \dot{Q}, \tag{2.4}$$

where $\nabla^2 = \vec{\nabla}\cdot\vec{\nabla}$ is the Laplace operator, here two-dimensional.

2.2. *BASIC SOLUTIONS*

The solution of (2.4) presented here is a generalization of the first literature solution, the Krogh equation [16]. The latter was for a radially

symmetric case, without Mb, solved for radial distance r between capillary radius r_c and outer radius R. This implies boundary conditions $p = p_c @ r = r_c$ and $dp/dr = 0 @ r = R$. Expressed in the current notation this so-called Krogh–Erlang equation reads

$$p = p_c + \frac{\dot{Q}}{4\mathscr{P}}\left[r^2 - r_c^2 - R^2 \ln\left(\frac{r^2}{r_c^2}\right)\right]. \tag{2.5}$$

The equation is valid only for $r_c \leqslant r \leqslant R$, but when extending the range to lower values of r it shows a singularity for $r \to 0$ [18]. This implies that there is a point-like oxygen source at $|\vec{r}| = 0$ (also see [1]). The oxygen supply area A_c of the source can be derived from integrating the radial flux $J_r = -\mathscr{P}\partial p^*/\partial r$ (see (2.2)) at an infinitesimal distance around the source:

$$\dot{Q}A_c = \lim_{r\to 0}\int_{-\pi}^{\pi} r d\phi J_r = \lim_{r\to 0}\int_{-\pi}^{\pi} r d\phi \frac{\dot{Q}}{2}\left\{\frac{R^2}{r} - r\right\} = \pi \dot{Q} R^2 \tag{2.6}$$

Note that the infinitesimal integral yields zero for all functions not having a singularity at $|\vec{r}| = 0$, such as the other terms in (2.5), so that always $R^2 = A_c/\pi$ and the generalization of (2.5) for N sources also in other geometries becomes straightforward:

$$p^* = \frac{\dot{Q}}{4\mathscr{P}}\left[\Phi(\vec{r}) - \sum_{i=1}^{N}\frac{A_i}{\pi}\ln\left(\frac{|\vec{r} - \vec{r}_i|^2}{r_{ci}^2}\right)\right], \tag{2.7}$$

where $\Phi(\vec{r})$ is a generalization of the nonsource terms in (2.5) and now facilitation by myoglobin is included. This "background function" $\Phi(\vec{r})$ is a solution of (2.4) without sources. A_i is the supply area of the ith source, $\vec{r}_i$ its location, and r_{ci} is a characteristic distance (to make the logarithm term dimensionless; e.g., capillary radius). The supply areas no longer need to be circular like in the Krogh model (see [11, fig. 4]). The sources are point-like and will deliver O_2 into their surroundings including the capillary itself; mostly, this will be a negligible fraction of A_i. Also, it is allowed that A_i be negative, implying that the "source" draws O_2 from its vicinity. That could occur, e.g., for very low oxygen pressure in such a capillary.

2.3. *BACKGROUND FUNCTION*

The background function $\Phi(\vec{r})$ is solved from the nonhomogeneous equation (2.4) and consequently can be split into a specific part $\Phi_S(\vec{r})$

and a homogeneous, harmonic part $\Phi_H(\vec{r})$:

$$\Phi(\vec{r}) = \Phi_S(\vec{r}) + \Phi_H(\vec{r}) \begin{cases} \nabla^2 \Phi_S = 4 \\ \nabla^2 \Phi_H = 0 \end{cases}. \tag{2.8}$$

A solution for the specific part can be constructed as

$$\Phi_S(\vec{r}) = \int_A \int \frac{d\vec{r}'}{\pi} \ln\left(\frac{|\vec{r} - \vec{r}'|^2}{r_s^2} \right) \tag{2.9}$$

as can be easily verified from Green's theorem [22]. In this equation, A is the area where the oxygen is consumed and r_s is a generalized normalization factor to make the term in the logarithm dimensionless. This leaves the problem of the boundary conditions to the solution of the homogenous part $\Phi_H(\vec{r})$. Depending on external circumstances, any harmonic function could be a potential solution for $\Phi_H(\vec{r})$. We will argue in Section 2.4 that the particular solution where $\Phi_H(\vec{r})$ is a constant is compatible with a most feasible set of boundary conditions, representative for a tissue portion embedded in a bulk of surrounding tissue.

There are some cases of particular interest for the specific solution $\Phi_S(\vec{r})$ that will be explicitly solved here.

2.3.1. *Circular Consumption Field*

A circle around the origin with radius R is a circular consumption field. In this case, we have, expressed in two-dimensional circular coordinates (r, ϕ):

$$\Phi_S(r, \phi) = \int_0^R dr' r' \int_{-\pi}^{\pi} d\phi' \frac{1}{\pi} \ln\left(\frac{r^2 - 2rr' \cos(\phi - \phi') + r'^2}{r_s^2} \right) \tag{2.10}$$

for which the solution is, choosing $r_s^2 = R^2/e$ (see Appendix 1):

$$\Phi_S(r, \phi) = \begin{cases} r^2 & r < R \\ R^2\{\ln(r^2/R^2) + 1\} & r > R \end{cases}. \tag{2.11}$$

2.3.2. *Rectangular Consumption Field*

Then, in terms of cartesian coordinates (x, y):

$$\Phi_S(x, y) = \int_{-\frac{1}{2}w}^{\frac{1}{2}w} dx' \int_{-\frac{1}{2}h}^{\frac{1}{2}h} dy' \frac{1}{\pi} \ln\left(\frac{(x - x')^2 + (y - y')^2}{r_s^2} \right), \tag{2.12}$$

where w, h are width and height of the rectangle, respectively, and the origin is at the center. Again choosing r_s appropriately, this can be written as (see Appendix 2):

$$\Phi_S(x,y) = \frac{1}{\pi} \sum_{m=1}^{4} \left\{ \Delta x_m \Delta y_m \ln\left(\frac{\Delta x_m^2 + \Delta y_m^2}{w^2 + h^2} \right) + \Delta x_m^2 \arctan\left(\frac{\Delta y_m}{\Delta x_m} \right) + \Delta y_m^2 \arctan\left(\frac{\Delta x_m}{\Delta y_m} \right) \right\}, \tag{2.13}$$

where the arctangent is defined yielding values in the interval $(-{}^1/_2\pi, {}^1/_2\pi)$ and $\Delta x_1 = \Delta x_2 = {}^1/_2 w - x$, $\Delta x_3 = \Delta x_4 = {}^1/_2 w + x$, $\Delta y_1 = \Delta y_4 = {}^1/_2 h - y$, $\Delta y_2 = \Delta y_3 = {}^1/_2 h + y$ are the distances to the four corner points. By adding the limit values for $\Delta x_m \to 0$ and $\Delta y_m \to 0$ the solution is defined and valid over the entire x, y plane both inside and outside the rectangle.

2.3.3. *Combined Solutions*

Because of linearity, combinations of the above particular solutions (2.11), (2.13) can be used for an area consisting of zones with constant but different consumption. As an example, when a circular area has two zones, a circular inner zone up to $r = R_I$ with consumption $f_I \dot{Q}$ and a ring-shaped outer zone $R_I < r < R$ with consumption $f_O Q$, the solution becomes

$$\Phi_S(r,\phi) = \begin{cases} f_I r^2 & r < R_I \\ f_O r^2 + (f_I - f_O) R_I^2 \{\ln(r^2/R_I^2) + 1\} & R_I < r < R \\ f_O R^2 \{\ln(r^2/R^2) + 1\} & \\ \quad + (f_I - f_O) R_I^2 \{\ln(r^2/R_I^2) + 1\} & r > R \end{cases}.$$

Also, extending the range of possibilities for calculating realistic tissue situations, the following possibilities should be mentioned:

2.3.4. *Field with Inhomogeneous Consumption*

In fact, this implies that consumption is not overall constant but can vary with location $\vec{r}$. This means that in (2.4) $\dot{Q}$ has to be replaced by $\dot{Q} g_s(\vec{r})$, where the average value of the weight function $g_s(\vec{r})$ over the

whole area is 1. Modifying (2.9) the corresponding solution for $\Phi_S(\vec{r})$ now reads

$$\Phi_S(\vec{r}) = \int_A \int \frac{d\vec{r}'}{\pi} g_s(\vec{r}') \ln\left(\frac{|\vec{r} - \vec{r}'|^2}{r_s^2} \right). \tag{2.14}$$

2.3.5. *Field with Distinct Consuming Sources*

The main reason that tissue consumption can depend on location is because the consuming entities, the mitochondria, are inhomogeneously distributed. Equation (2.14) can be discretized to account for these individual oxygen sinks:

$$\Phi_S(\vec{r}) = \sum_{j=1}^{N^\cdot} \frac{A_j^\cdot}{\pi} \ln\left(\frac{|\vec{r} - \vec{r}_j^\cdot|^2}{r_{sj}^2} \right), \tag{2.15}$$

where there are $N^\cdot$ sinks and $A_j^\cdot$, $\vec{r}_j^\cdot$ and r_{sj} are demand area, location, and normalization factor of the jth sink, respectively. Again, (2.4) should be modified accordingly. Note, that in fact the mitochondria are treated here as infinitesimal sinks, analogous to the infinitesimal sources in (2.7).

2.4. *BOUNDARY CONDITIONS*

It is straightforward to choose a set of boundary conditions on the following assumptions:

(1) tissue pO_2 near the kth capillary is imposed by the capillary pO_2;

(2) the tissue slab under consideration is representative, without bulk external O_2 fluxes going in or out.

For an extensive discussion about boundary conditions see [20].

Elaborating (1) we will assume a certain value for the capillary, or, better, the erythrocyte O_2 pressure p_{ck} which has to be related to the local tissue value. Average tissue pO_2 around the capillary must be obtained from (2.7) integrated along the capillary outline, denoted by rim k:

$$p_{rk}^* = \frac{\oint_{\text{rim } k} d\vec{r} p^*(\vec{r})}{\oint_{\text{rim } k} d\vec{r}}. \tag{2.16}$$

For all the terms in (2.7), this integral can easily be calculated if the capillary outline is treated as a circle with its center at $\vec{r}_k$ and radius r_{ck}. For the harmonic terms in (2.7), e.g., the source terms of the other capillaries ($i \neq k$), the circular integral equals $2\pi r_{ck}$ times the value at $\vec{r} = \vec{r}_k$ [22]. $\Phi_S(\vec{r})$ can be written as a harmonic function plus the specific solution $|\vec{r} - \vec{r}_k|^2$ (analogous to the partition in (2.8)) and the kth source itself vanishes because $|\vec{r} - \vec{r}_k| = r_{ck}$:

$$p^*_{rk} = \frac{\dot{Q}}{4\mathscr{P}} \left\{ \Phi(\vec{r}_k) + r^2_{ck} - \sum_{\substack{i=1 \\ i \neq k}}^{N} \frac{A_i}{\pi} \ln\left(\frac{|\vec{r}_k - \vec{r}_i|^2}{r^2_{ci}} \right) \right\}. \tag{2.17}$$

Using (2.3), an equilibrium oxygen pressure p_{rk} can be calculated from p^*_{rk}. However, this "rim value" p_{rk} in general will not be equal to the capillary, or, better, the erythrocyte, value p_{ck}. The main reason is that there is a pressure drop due to transport within the blood up to the capillary rim [6, 9, 20]. But also, there is disequilibrium between oxygen and oxymyoglobin—the gradient in cO_2Mb and consequently in s is zero while the gradient in p^* is not [4, 5]. As a first approximation we will assume that the difference between p_{rk} and p_{ck} is linearly proportional to the average O_2 flux across the capillary rim. The same was done by [3] who termed this proportionality constant the "mass transfer coefficient." The average O_2 flux is linearly proportional to the O_2 supply area A_k (see first part of (2.6)) and consequently the difference between p_{rk} and p_{ck} is also [9, 11]:

$$\begin{aligned} p^*_{rk} &= p_{rk} + p_F s(p_{rk}) \\ p_{rk} &= p_{ck} - \gamma_k A_k, \end{aligned} \tag{2.18}$$

where γ_k is the proportionality constant (the averaged pressure difference $\sum_k \gamma_k A_k / N$ sometimes is referred to as *extraction pressure* or *capillary barrier* [6, 25]) and s is written as a function of p:

$$s(p) = \frac{p}{p_{50} + p},$$

where p_{50} is the myoglobin half-saturation pressure.

Assumption (2) should impose constraints on the background function $\Phi(\vec{r})$ and in particular on the homogeneous part $\Phi_H(\vec{r})$. Most authors impose boundary conditions either on p at the border of the

region under consideration or on its gradient across this border. When there is no gradient of p across the border, the region is not influenced by what is outside, and vice versa. But this is not realistic for a part of a tissue embedded in a larger entity; there *will* be fluxes in and out, in particular for irregular capillary (sources) distribution. That should occur in such a way that the tissue parts do not influence each other globally. This is explained and elaborated in Appendix 3; the outcome is that the constraint of no flux across the border should be imposed on the homogeneous part of the background function $\Phi_H(\vec{r})$. This homogeneous part is what remains when both sources, the ln( )-terms in (2.7) and tissue consumption terms $\Phi_S(\vec{r})$, are removed and it should not be influenced by the outside world. The solution of (2.8) for zero gradient of $\Phi_H(\vec{r})$ around the whole border is a constant, denoted by Φ_0 [22]. Also as a consequence, total O_2 supply area must balance total consumption area:

$$A = \sum_{i=1}^{N} A_i, \tag{2.19}$$

where A is the total area of the consuming slab (averaged over consumption if there are zones with different consumption).

3. CALCULATION ALGORITHMS

For solving Φ_0, A_i in an actual situation, an iterative procedure can be set up; this can be done in terms of a linearized set of equations. Let us assume that there are estimates of these values, denoted by $\Phi_0^{(j)}$, $A_i^{(j)}$. When inserted into (2.17), these estimates will lead to a value for p_{rk}^* that will be different from the value obtained from (2.18). To distinguish between these, we will add a subscript 1 for the result of (2.17) and a subscript 2 for the result of (2.18):

$$p_{rk,1}^{*(j+1)} = p_{rk,1}^{*(j)} + \frac{\dot{Q}}{4\mathscr{P}}\left\{\Phi_0^{(j+1)} - \Phi_0^{(j)} - \sum_{\substack{i=1 \\ i\neq k}}^{N} \frac{A_i^{(j+1)} - A_i^{(j)}}{\pi} \ln\left(\frac{|\vec{r}_k - \vec{r}_i|^2}{r_{ci}^2}\right)\right\}$$

$$p_{rk,2}^{*(j+1)} \approx p_{rk,2}^{*(j)} - \gamma_k\left(1 + p_F \frac{ds}{dp}\left(p_{rk}^{(j)}\right)\right)\left(A_k^{(j+1)} - A_k^{(j)}\right),$$

where the second formula is a first-order Taylor expansion around $p_{rk}^{(j)}$. The next step should be taken such that the expected values of $p_{rk,1}^{*(j+1)}$ and $p_{rk,2}^{*(j+1)}$ are equal. This leads to N linear equations

$(k = 1,\ldots,N)$ where there are $N+1$ unknowns Φ_0, A_k. The additional linear equation $(k = 0)$ is obtained from (2.19):

$$0 = \sum_{i=1}^{N} A_i^{(j+1)} - A_i^{(j)} \tag{3.1}$$

so that we have a complete set which can be expressed in terms of a $(N+1)\times(N+1)$ matrix equation:

$$\sum_{i=0}^{N} \underline{\mathbf{M}}_{ki} U_i = V_k; \qquad 0 \leqslant k \leqslant N,$$

where

$$\underline{\mathbf{M}}_{00} = 0$$

$$\underline{\mathbf{M}}_{0i} = 1 \qquad 1 \leqslant i \leqslant N$$

$$\underline{\mathbf{M}}_{k0} = 1 \qquad 1 \leqslant k \leqslant N$$

$$\underline{\mathbf{M}}_{ki} = -\ln\left(\frac{|\vec{r}_k - \vec{r}_i|^2}{r_{ci}^2}\right) \qquad 1 \leqslant i \neq k \leqslant N$$

$$\underline{\mathbf{M}}_{kk} = \frac{4\pi\mathscr{P}\gamma_k}{\dot{Q}}\left(1 + p_F \frac{ds}{dp}\left(p_{rk}^{(j)}\right)\right) \qquad 1 \leqslant k \leqslant N$$

$$U_i = \begin{cases} \pi\left(\Phi_0^{(j+1)} - \Phi_0^{(j)}\right) & i = 0 \\ A_i^{(j+1)} - A_i^{(j)} & 1 \leqslant i \leqslant N \end{cases}$$

$$V_k = \begin{cases} 0 & k = 0 \\ \dfrac{4\pi\mathscr{P}}{\dot{Q}}\left\{p_{rk,2}^{*(j)} - p_{rk,1}^{*(j)}\right\} & 1 \leqslant k \leqslant N. \end{cases}$$

Note that the matrix depends on the former estimates $\Phi_0^{(j)}, A_i^{(j)}$ only if at least one γ_k is nonzero. If the assumption is allowed that all γ_k's are zero, the above treatment yields final values of Φ_0 and A_i directly, in one step, whereas for nonzero γ_k the calculation procedure has to be iterated. For the initial guesses, in order to obey (3.1) we have to choose the supply areas such that (2.19) is fulfilled, e.g.,

$$A_i^{(0)} = \frac{A}{N},$$

whereas $\Phi_0^{(0)}$ in principle can be chosen arbitrarily, e.g., calculated equating (2.17) to (2.18) for one selected capillary.

A strict proof of the convergence of the iteration procedure is not given here, but in the practical cases considered so far, three iterations were sufficient.

4. EXAMPLE

As a calculation example, the capillary arrangement of Figure 1 was chosen. Throughout the example, both distances and pressures will be expressed as fractions of the maximum (0–1). A rectangular field is divided into four zones of equal size with different conditions of capillary spacing/capillary pO_2, as indicated by the letter combinations in Figure 1. The first letter **E** or **H** indicates equally or heterogeneously spaced capillaries and the second letter **I** or **R** identical or randomly distributed capillary pO_2, respectively (the identical pressure value being the mean of the random values). The equally spaced capillaries were placed in a filled hexagonal grid whereas the heterogeneous distances were as for realistic rat heart with a capillary radius of 0.0158 for each capillary. Mean capillary pO_2 was 0.61 and standard deviation

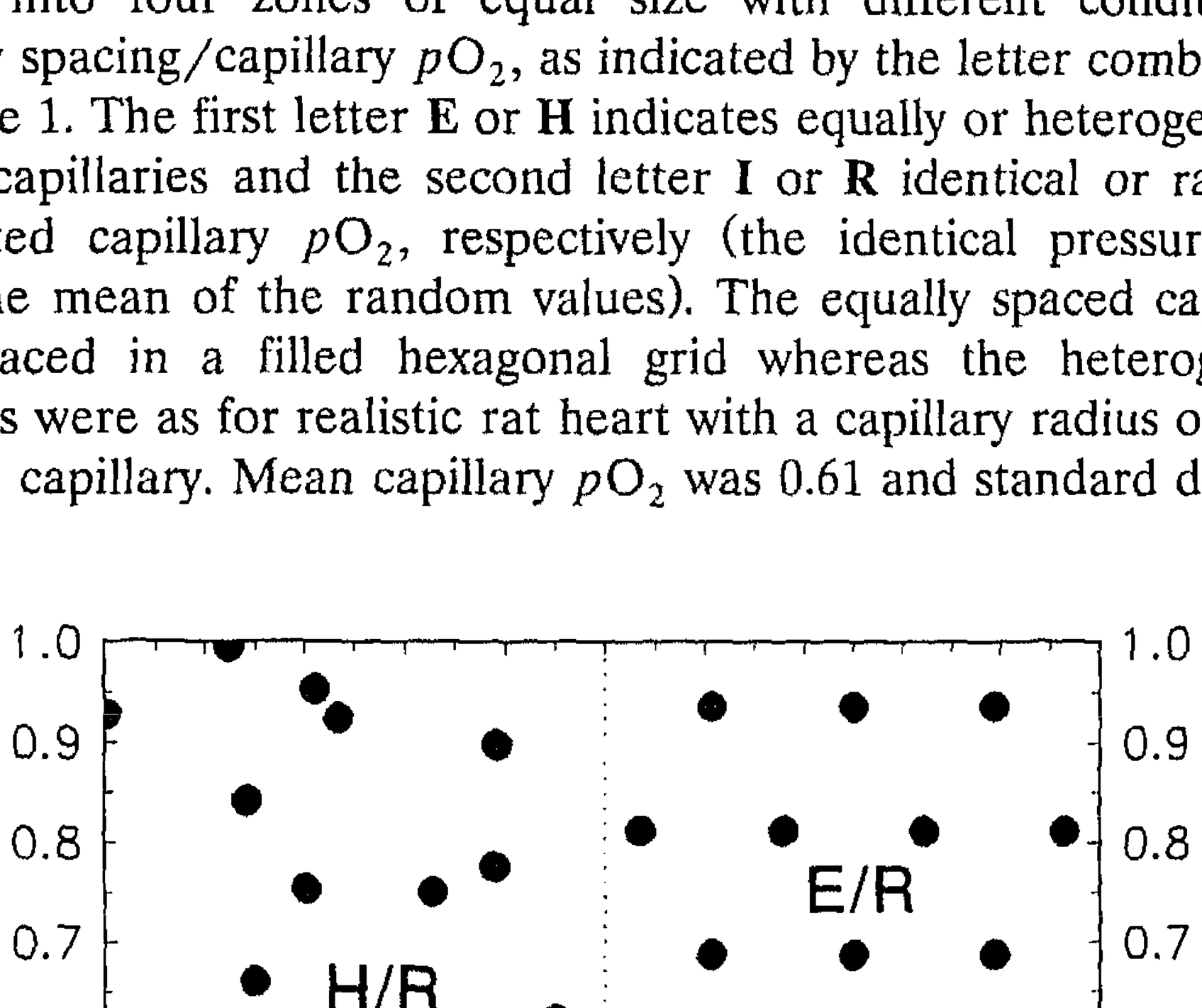

FIG. 1. Capillary locations of an exemplary case. A square field composed of four square zones with different capillary properties as indicated by the two-letter coding. The first letter indicates equal (**E**) or heterogeneous (**H**) capillary spacing, the second identical (**I**) or randomly distributed (**R**) capillary pO_2. Distances are given as fractions of the maximum distance. The arrow indicates the viewpoint direction of Figure 2.

(SD) of the random distribution was 0.21 (note that all values are expressed as fractions of the maximum value of 1). In these units, $\dot{Q}/\mathscr{P}$ was 72.2 (pressure/length^2). The actual data are from [11] combined with rectangle size of 152 μm ($r_c = 0.0158 \times 152$ μm $= 2.4$ μm) and a mean capillary pO_2 of 8 kPa. Both p_F and all γ_k were chosen zero. The example is to elucidate the effects of capillary heterogeneities.

First Φ_0 and A_i were calculated as described in Section 3. The initial Φ_0 was chosen zero; no iterations were needed since $\gamma_k \equiv 0$ here. Some characteristics of the resulting A_i are given in Table 1, expressed in fractions of the overall average area size $A/N = 1/56$. Clearly, in the doubly homogeneous zone **E/I** supply areas are the most uniform. One very small area is present in the **E/R** zone; note that a negative supply area is not excluded by the theoretical treatment. A negative supply area implies inflow of oxygen into the capillary and this should be allowed for a very low capillary pO_2, lower than that of the surrounding tissue. Note that the respective zone is one of random capillary pO_2.

This is further illustrated in Figure 2, calculated through (2.7) for the rectangular field, (2.13). In a three-dimensional plot, pO_2 is shown on the vertical axis against location in the rectangular field (ground plane). The viewpoint is from the direction of the **E/I** zone ($-45°$ as indicated by the thick arrow in Figure 1) and 45° above the ground plane. Capillary pO_2's are shown as black dots; because $\gamma_k \equiv 0$ these values must match tissue capillary rim pO_2 which is nicely obeyed as seen from the figure. Each dot is on top of an "oxygen hill," where the O_2 flows into the supply area. The capillaries in the front **E/I** zone, with both homogeneous distance and pO_2, have almost equal "hills." Either heterogeneity in spacing or in capillary pressure leads to different shapes and sizes of the "hills"; the resulting variation in supply area is also clearly visible. The lowest A_i value of 0.11 occurs in the right **E/R** zone just besides the front **E/I** zone, where a capillary happens to have a very low pO_2 of 0.26 amidst adjacent high values.

TABLE 1

Summary of Calculated O_2 Supply Areas for the Example of Figure 1*

NA_i/A	**E/I**	**E/R**	**H/R**	**H/I**
Minimum	0.76	0.11	0.31	0.53
Maximum	1.23	1.86	1.50	1.48
Mean	1.01	1.02	0.96	1.01
SD	0.10	0.49	0.44	0.33

*Zones indicated as in that figure. Minimum, maximum, mean, and standard deviation (SD) for each zone were expressed as fractions of the overall average ara size ($1/N$ where $N = 56$).

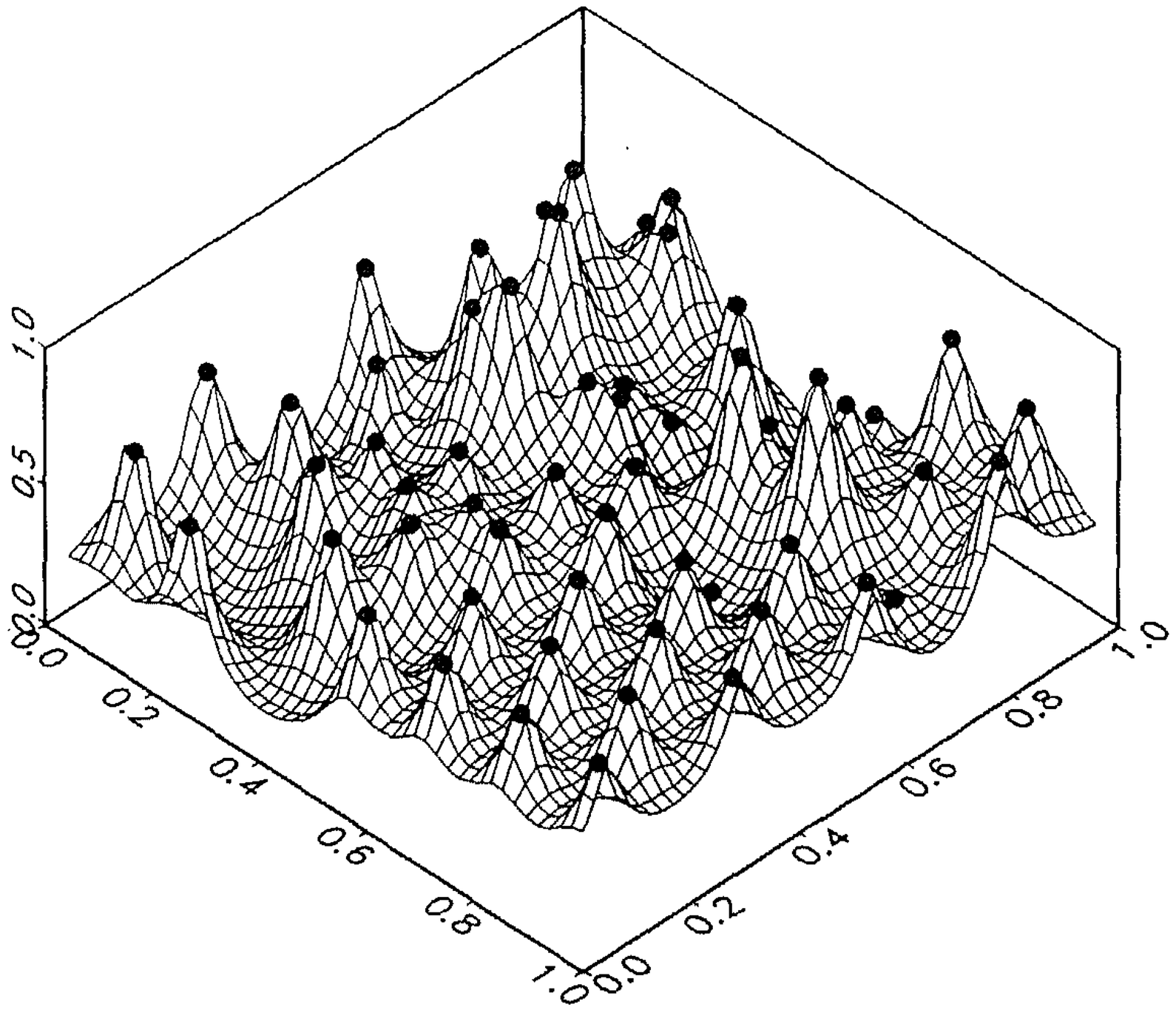

FIG. 2. Tissue pO_2 (vertical axis; relative units) field calculated for the capillary rangement of Figure 1; ground plane shown with the same axes as in this figure E/I zone in front as indicated by the arrow there). Solid dots indicate capillary ressure.

. DISCUSSION

The above treatment yields an analytical solution for two-dimensional O_2 diffusional transport under the conditions as set out here. his two-dimensional transport does not exclude O_2 gradients in the -direction perpendicular to the plane; merely, in the Laplace operator ^{2} the term $\partial^2/\partial z^2$ must be negligible. This constraint is not examned here, but in the comparable Krogh model—two-dimensional diffuion in a single-capillary tissue cylinder—it turns out to be a valuable pproximation [14].

The solution is exact under the conditions mentioned, which can be ummarized as follows:

(1) Local conditions
   (i) the capillary can be represented by a single point source;
   (ii) the capillary pO_2 boundary condition can be treated as described in Section 2.4, i.e., tissue pO_2 is equal to a linear combination of capillary pO_2 (averaged over circular out-

line) and capillary O_2 supply (expressed in supply area A_k); this capillary boundary condition includes correction for disequilibrium between pO_2 and myoglobin saturation;

(2) Global conditions

(i) tissue can be considered homogeneous with respect to O_2 diffusion, i.e., $\mathscr{P}, p_F$ must be constants over the region considered;

(ii) global oxygen consumption equals oxygen supply resulting in (2.19);

(iii) the "background function" $\Phi(\vec{r})$ must be solved from additional boundary conditions. Here, $\Phi(\vec{r})$ is split into a specific and a homogeneous part according to (2.8) and

(a) $\Phi_S(\vec{r})$ can be calculated from the assembled O_2 sinks, (2.9) (homogeneous consumption) or (2.14) or (2.15);

(b) $\Phi_H(\vec{r})$ has zero gradient across the boundary of the area considered. This leads to the solution that $\Phi_H(\vec{r})$ equals a constant Φ_0.

(3) Steady state.

Note that the basic solution (2.7) does not rely on an overall constant $\dot{Q}$ but that variable $\dot{Q}$ can be accounted for by taking a representative (e.g., average) constant $\dot{Q}$ in (2.7) and accounting for varying consumption in solving for $\Phi(\vec{r})$ and A_i. How to do that for $\Phi(\vec{r})$ is set out in (2.8), (2.9) and (2.14), (2.15); the A_i follow from solving for the boundary conditions. Also note, that (2.15) allows for consumption to be modeled as a set of N^* discrete sinks, for which read: mitochondria. The further examples, circular (2.11) or rectangular (2.13) field, are elaborations for homogeneous consumption. The picture changes somewhat if consumption $\dot{Q}$ is not determined by local conditions but depends on oxygen pressure p. Then, if p is known for any location (x, y), $\dot{Q}$ can be represented as locally dependent and in turn p calculated; this should yield the same p field. For such a scheme an iterative procedure could be developed.

Considering the local conditions (1)(i) and (1)(ii), there is little to say about these without solving for the O_2 transport situation in the capillary itself. Apart from this being a difficult time-dependent three-dimensional problem, it is not an objective of the present investigation. It is a known fact, however, that "far away" from a source this source always "resembles" a point source; in terms of the treatment here, the point source term $A_i \ln(|\vec{r} - \vec{r}_i|^2 / r_{ci}^2)$ can be generalized as

$$\int_{A_i} \int d\vec{r}' g_{ci}(\vec{r}') \ln\left(\frac{|\vec{r} - \vec{r}'|^2}{r_{ci}^2} \right),$$

re the integration is over the capillary area and $g_{ci}(\vec{r})$ is a dimen-
lless weight function. For large values of $|\vec{r}-\vec{r}_i|$, a Taylor expansion
ınd $\vec{r}'' = \vec{r}' - \vec{r}_i$ leads to:

$$\left[\int_{A_i}\int d\vec{r}''\, g_{ci}(\vec{r}_i+\vec{r}'')\right]\ln\left(\frac{|\vec{r}-\vec{r}_i|^2}{r_{ci}^2}\right)$$

$$-2\int_{A_i}\int d\vec{r}''\, g_{ci}(\vec{r}_i+\vec{r}'')\frac{(\vec{r}-\vec{r}_i)\cdot\vec{r}''}{|\vec{r}-\vec{r}_i|^2}+\cdots,$$

e term between brackets is A_i, the second term can be made zero by appropriate choice of $\vec{r}_i$ and the other terms are of order $|\vec{r}-\vec{r}_i|^{-2}$ less. As a consequence, the approximation is expected to be less good en close to a capillary.

Note that (2.4) is valid only outside the capillaries. In fact, (2.7) is a ution of an extended equation with Dirac-delta functions on the ırces, as pointed out by [18]. On the other hand, $\Phi(\vec{r})$ is valid in the ole plane—it is independent of the sources.

The global conditions (2)(ii) and (2)(iii) are ready conditions for a tistically representative portion of tissue not subject to external luences. With these, the solution should be inherently independent of e and location of the area considered, as long as it is large enough to representative [11]. The above treatment, however, is open to exten-ıns. For example, when a tissue is near to an external O_2 source (like e heart wall) there can be global in/outflow of oxygen. This can be ken into account in the boundary conditions for the harmonic func-ın $\Phi_H(\vec{r})$ of (2.8) and in the boundary condition equalling global pply and consumption, (2.19). The first must be solved differently ɔm the constant Φ_0 of the above treatment, while the second must be odified to account for an effective area size A_E into which the ternal source transfers oxygen.

Global condition (2)(i) is a more awkward one. The above treatment ems no longer appropriate for varying or discontinuous $\mathscr{P}, p_F$ since e differential equation (2.4) will have to be extended at least with rms like $(\nabla\mathscr{P})\cdot(\nabla p)$ and a solution of type (2.7) is of questionable ılue. Undoubtedly, tissue has heterogeneous O_2 diffusion properties ıt it is unclear how important this is. From an external global view, verall parameters can be derived representing tissue and even blood as ɔmogeneous [23]; locally, however, there may remain differences. ocal discontinuities in $\mathscr{P}, p_F$ can be modeled in simplified tissue ıyouts, e.g., concentric tissue cylinders [10], showing only minor influ-

ence on p. Also given the fact that experimental data are virtually lacking, treating the tissue using these overall global parameters might be a good method.

The assumption (3), of steady state, in fact should be read as "quasisteady state." It is for a situation that should be maintained as local average over a certain time. Rapid oscillations (e.g., due to erythrocytes passing by in the capillaries) might be superimposed on the steady-state solution; long-time effects like gradual shifts in capillary O_2 supply (e.g., due to changing capillary flow) might be modeled as gradual shifts from one almost-steady state to another. In both instances, the above solution can serve as a basis for further extension.

Many aspects of the present solution are already found in earlier modeling of tissue oxygenation. Ultimately, it can be considered as an extension of the Krogh model [6, 16]. Extending to multiple point-like sources was proposed by Popel [18]. This author also pointed out that such a solution is incompatible with capillary boundary conditions and that instead an average capillary rim value must be used—his Equation (14) is equivalent to (2.16) of the present treatment. Heterogeneity of capillary locations was solved numerically [2]. Clark et al. [1] also added superposition of sources in an analytical model but did not link the oxygen supply areas to capillary pO_2's. Instead, chosen distributions of their "capillary production rate" γ_{ck} (equivalent to our A_k) were used for the calculations. Here, the A_k are calculated from the actual conditions. This involves a "loss in pO_2" due to transport from the erythrocyte towards but only up to the tissue. The same concept is found in [3]; their "mass transfer coefficient" k is related to our γ_i by the approximate equation $2\pi k\gamma_i r_{ci} \approx \dot{Q}$.

Most models use exact boundary conditions, often in terms of zero pO_2 or zero flux at the outline of the region considered. Zero flux with a rectangular region applies when the region can be repeated periodically (see [20]). Zero flux with a circular region can be handled analytically [1, 22]. Here, oxygen is allowed to flow out of and into the region, just as will happen in reality. A capillary near the border will supply some O_2 to tissue just outside the field under consideration, whereas a capillary close to but outside this region will send some O_2 in. The net amount of O_2 crossing the border should be zero, (2.19).

The present solution can be used either as a basis for a three-dimensional solution by superposition of layers (see [6, 13, 20]), or directly, for a layer with known capillary pO_2's. For example, when from a photomicrograph of a tissue cross-section capillary locations and capillary erythrocyte saturations can be determined, the model might be applied directly. If the tissue slice is representative, a representative pO_2 histogram should result.

The example of the Section 4 was chosen as an illustration of the impact of the solution. In particular, the influence of heterogeneities in position and pO_2 of the capillary was stressed. Tissue situations can be very different, leading to very different results for pO_2 distribution [8, 25]. Another important heterogeneity considered in the literature is that of capillary flow [2, 8, 19, 20]; for this, however, a three-dimensional model is needed.

The power of the present treatment is that it yields a direct analytical solution in cases where an otherwise complex numerical approach would be needed. In order for the tissue portion to be representative, it should encompass at least several tens of capillaries [11]. Because of local high gradients (see Figure 2) the calculation grid should be small or complex, resulting in a large number of computations. Capillary pO_2 is not easily translated into grid boundary conditions. O_2 supply areas are not readily calculated in a numerical scheme and consequently condition (2.19) cannot be used; replacing it with a condition like zero flux at the boundaries results in mixed boundary conditions. Last but not least, numerical schemes are not so open to extensions towards other situations, e.g., three-dimensional diffusion or external O_2 supply. The present treatment is capable of serving as a basis for that.

APPENDIX 1

First, we define the function:

$$F(s) = \int_{-\pi}^{\pi} s\,d\alpha\,\ln\{1-2s\cos(\alpha)+s^2\}.$$

In the domain $0 \leqslant s < 1$ this is a circular integral with radius s over a harmonic function, so equal to 2π times this radius times the function limit value for zero radius [22]:

$$F(s) = 2\pi s \ln(1) = 0; \qquad 0 \leqslant s < 1.$$

Then, the function is also easily found for $s > 1$:

$$F(s) = \int_{-\pi}^{\pi} s\,d\alpha\,\ln(s^2) + s^2 F(1/s) = 2\pi s \ln(s^2); \qquad s > 1$$

In terms of this function, (2.10) now can be written as

$$\Phi_S(r,\phi) = \int_0^R dr'\,r' \int_{-\pi}^{\pi} d\phi'\,\frac{1}{\pi}\ln\left(\frac{r^2}{r_s^2}\right) + \frac{1}{\pi}\int_0^R dr'\,rF(r'/r).$$

The first integral is solved easily as $R^2 \ln(r^2/r_s^2)$, whereas the second integral will be different for $r < R$ and for $r > R$. In the latter case, $r'/r < 1$ everywhere so that the result is zero. Otherwise, there is a region $r < r' < R$ where the integration is nonzero:

$$r < R: \int_0^R dr' rF(r'/r) = \int_r^R dr' 2\pi r' \ln\left(\frac{r'^2}{r^2}\right)$$
$$= \pi R^2 \left\{\ln\left(\frac{R^2}{r^2}\right) - 1\right\} + \pi r^2;$$

with these results and choosing $r_s^2 = e^{-1}R^2$, (2.11) is easily derived.

APPENDIX 2

For the solution of (2.12), the rectangular field, we will use the following two integrals:

$$\int ds \ln(s^2 + t^2) = s \ln(s^2 + t^2) - 2s + 2t \arctan\left(\frac{s}{t}\right) \qquad (A.1)$$

$$2\int ds\, s \arctan\left(\frac{t}{s}\right) = s^2 \arctan\left(\frac{t}{s}\right) - t^2 \arctan\left(\frac{s}{t}\right) + st \qquad (A.2)$$

for each combination of s, t; both equations can be easily verified by differentiation to s. The arctangent is defined yielding values in the interval $-{}^1/_2\pi \to {}^1/_2\pi$ and we will, at first, consider only positive values of s in the integration to avoid switching of the arctan from $-{}^1/_2\pi$ to $+{}^1/_2\pi$ when s crosses zero. This means, that we can solve (2.12) for the quadrant $x < -{}^1/_2 w$, $y < -{}^1/_2 h$, using (A.1) substituting $s = (y' - y)/r_s$, $t = (x' - x)/r_s$:

$$\Phi_S(x,y) = \int_{-\frac{1}{2}w}^{\frac{1}{2}w} dx' \frac{1}{\pi}\left[(y'-y)\ln\left(\frac{(x'-x)^2+(y'-y)^2}{r_s^2}\right) - 2(y'-y)\right.$$
$$\left. + 2(x'-x)\arctan\left(\frac{y'-y}{x'-x}\right)\right]_{y'=-\frac{1}{2}h}^{y'=\frac{1}{2}h},$$

which can be worked out as, defining $\Delta y_1 = {}^1/_2 h - y$, $\Delta y_2 = {}^1/_2 h + y$ and using $\arctan(-s) = -\arctan(s)$:

$$\Phi_S(x,y) = \int_{-\frac{1}{2}w}^{\frac{1}{2}w} dx' \frac{1}{\pi} \sum_{m=1}^{2} \left\{\Delta y_m \ln\left(\frac{(x'-x)^2 + \Delta y_m^2}{r_s^2}\right)\right.$$
$$\left. - 2\Delta y_m + 2(x'-x)\arctan\left(\frac{\Delta y_m}{x'-x}\right)\right\}.$$

Next, we apply (A.1) and (A.2) now substituting $s=(x'-x)/r_s$, $t=\Delta y_n/r_s$ and proceed similarly to above, additionally defining $\Delta x_1=\Delta x_2={}^1/_2w-x$, $\Delta x_3=\Delta x_4={}^1/_2w+x$, $\Delta y_4=\Delta y_1$, $\Delta y_3=\Delta y_2$:

$$\Phi_S(x,y)=\frac{1}{\pi}\sum_{m=1}^{4}\left\{\Delta x_m\,\Delta y_m\ln\left(\frac{\Delta x_m^2+\Delta y_m^2}{r_s^2}\right)+\Delta x_m^2\arctan\left(\frac{\Delta y_m}{\Delta x_m}\right)+\Delta y_m^2\arctan\left(\frac{\Delta x_m}{\Delta y_m}\right)-3\Delta x_m\,\Delta y_m\right\}.$$

Since the sum over $\Delta x_m\,\Delta y_m$ is equal to wh, a constant, an appropriate choice of r_s^2 leads to (2.13). However, this solution was derived for only one quadrant outside the rectangle. For other values of x, y, the solution can proceed along the same lines but some more scrutiny is needed since $\arctan(t/s)$ takes a step of $\pm\pi$ when s goes across the value zero. The latter will be the case at the border lines of the rectangle: $\Delta x_m=0$ or $\Delta y_m=0$, for each m. By adding the limit value, however, the solution (2.13) can be made continuously differentiable since the undetermined value of the arctangent, $+{}^1/_2\pi$ or $-{}^1/_2\pi$, is multiplied by zero even in the first derivative. Consequently, (2.13) is valid for the whole x, y plane, as can be verified by elaborating the above procedure also for these other values of x and y.

APPENDIX 3

The logarithm terms as they are in (2.7) and (2.9) (and also (2.14) and (2.15)) can be expanded for large values of $|\vec{r}|$, $|\vec{r}|\gg|\vec{r}''|$, as

$$\ln\left(\frac{|\vec{r}-\vec{r}''|^2}{r_s^2}\right)\Rightarrow\ln\left(\frac{|\vec{r}|^2}{r_s^2}\right)-2\frac{\vec{r}\cdot\vec{r}''}{|\vec{r}|^2}+\cdots,$$

in particular, for (2.9):

$$\Phi_S(\vec{r})\Rightarrow\frac{A}{\pi}\ln\left(\frac{|\vec{r}|^2}{r_s^2}\right)-\frac{2\vec{r}}{\pi|\vec{r}|^2}\cdot\int_A\int d\vec{r}\,'\vec{r}\,'+\cdots,$$

where the second term in the expansion is of order $|\vec{r}|^{-1}$ and the remaining terms are of order $|\vec{r}|^{-2}$ or smaller. Accordingly, (2.7) can be worked out as

$$p^*\Rightarrow\frac{\dot{Q}}{4\mathscr{P}}\left[\Phi_H(\vec{r})-\sum_{i=1}^{N}\frac{A_i}{\pi}\ln\left(\frac{r_s^2}{r_{ci}^2}\right)+\frac{1}{\pi}\ln\left(\frac{|\vec{r}|^2}{r_s^2}\right)\left\{A-\sum_{i=1}^{N}A_i\right\}+\frac{2\vec{r}}{\pi|\vec{r}|^2}\left\{\sum_{i=1}^{N}A_i\vec{r}_i-\int_A\int d\vec{r}\,'\vec{r}\,'\right\}+\cdots\right],$$

which means that the summed contribution of consumption and sources vanishes if the amount of oxygen consumed is equal to the amount released by the sources ((2.19)) and even faster when the sources are statistically neatly distributed $-\sum A_i \vec{r}_i = \int\int d\vec{r}\,' \vec{r}\,'$. The remaining part is made up by the harmonic part of the background function $\Phi_H(\vec{r})$ so what the bulk of the tissue "sees" from this mathematical description is this $\Phi_H(\vec{r})$, the "global view" referred to in Section 2.4. Consequently, the corresponding boundary conditions should be imposed on $\Phi_H(\vec{r})$. Boundary conditions are common for the tissue part considered and for the surrounding bulk of tissue. If, as imposed in Section 2.4, it is like there is no flux in or out of the piece of tissue under consideration, the noflux boundary condition applies to $\Phi_H(\vec{r})$ and the only remaining solution is that it is a constant Φ_0.

APPENDIX 4: NOMENCLATURE

A	field area
A_c A_i A_k	capillary supply area
A_j	sink area
c	concentration
c_tMb	total myoglobin concentration
D	diffusion coefficient
f_I	consumption ratio of inner circular region
f_O	consumption ratio of outer ring
$g_{ci}(\vec{r})$	relative source strength
$g_s(\vec{r})$	relative sink strength
h	height of rectangular field
Hb	hemoglobin
$\vec{J}$	flux vector
J_r	radial flux component
$\underline{\mathbf{M}}$	matrix in the iteration procedure
Mb	myoglobin
N	number of capillaries
N_s	number of sinks
O_2Mb	oxymyoglobin
$\mathscr{P}$	oxygen permeability constant
p	oxygen partial pressure, pO_2
p_{50}	myoglobin half-saturation pressure
p_c p_{ck}	capillary oxygen pressure
p_F	facilitation pressure
p_{rk}	capillary rim pressure
p^*	oxygen driving pressure
p^*_{rk}	capillary rim driving pressure

$\dot{Q}$	oxygen consumption rate
R	cylinder/circle radius
R_1	radius of inner circle
r	radial coordinate
$\vec{r}$	two-dimensional coordinate vector
r_c r_{ci} r_{ck}	capillary radius or characteristic distance
$\vec{r}_i$ $\vec{r}_k$	capillary location
$\vec{r}_j$	sink location
r_s	generalized normalization distance
r_{sj}	sink normalization distance
rim k	capillary rim
s $s(p)$	*myoglobin saturation*
U V	vectors in the iteration procedure
w	width of rectangular field
X	arbitrary species
x y z	cartesian coordinates

Greek Symbols

αO_2	oxygen solubility
γ_k	pressure drop proportionality factor
Δx Δy	distances to corners in rectangular field
ϕ	angular coordinate
$\Phi(\vec{r})$	background function
Φ_0	constant background function
$\Phi_H(\vec{r})$	homogeneous part of background function
$\Phi_S(\vec{r})$	specific part of background function

Superscripts

(0) (j) (j+1)	iteration index
′ ″	dummy variable

REFERENCES

1 P. A. Clark, S. P. Kennedy, and A. Clark Jr., Buffering of muscle tissue PO_2 levels by the superposition of the oxygen field from many capillaries, in *Oxygen Transport to Tissue-XI*, Advances in Experimental Medicine and Biology, vol. 248, K. Rakušan, G. P. Biro, T. K. Goldstick, and Z. Turek, eds., Plenum Press, New York and London, 1989, pp. 165–174.

2 M. L. Ellsworth, A. S. Popel, and R. N. Pittman, Assessment and impact of heterogeneities of convective oxygen transport parameters in capillaries of striated muscle: Experimental and theoretical, *Microvasc. Res.* 35:341–362 (1988).

3 W. J. Federspiel and A. S. Popel, A theoretical analysis of the effect of the particulate nature of blood on oxygen release in capillaries, *Microvasc. Res.* 32:164–189 (1986).

4 J. E. Fletcher, On facilitated oxygen diffusion in muscle tissues, *Biophys. J.* 29:437–458 (1980).
5 L. Hoofd, Facilitated Diffusion of Oxygen in Tissue and Model Systems, Dissertation Thesis, University of Nijmegen, The Netherlands, 1987.
6 L. Hoofd, Updating the Krogh model—Assumptions and extensions, in *Oxygen Transport in Biological Systems*, Soc. Exper. Biol. Seminar Series 51, S. Egginton, and H. F. Ross, eds., Cambridge University Press, Cambridge, 1992, pp. 197–229.
7 L. Hoofd and F. Kreuzer, A new mathematical approach for solving carrier-facilitated steady-state diffusion problems, *J. Math. Biol.* 8:1–13 (1979).
8 L. Hoofd and Z. Turek, The influence of flow redistributions on the calculated pO_2 in rat heart tissue, in *Oxygen Transport to Tissue-XV*, Advances in Experimental Medicine and Biology, vol. 345, P. Vaupel, R. Zander, and D. F. Bruley, eds., Plenum Press, New York and London, 1993, pp. 275–282.
9 L. Hoofd, C. G. Bos, and Z. Turek, Modelling erythrocytes as point-like O_2 sources in a Kroghian cylinder model, in *Oxygen Transport to Tissue-XV*, Advances in Experimental Medicine and Biology, vol. 345, P. Vaupel, R. Zander, and D. F. Bruley, eds., Plenum Press, New York and London, 1993, pp. 893–900.
10 L. Hoofd, Z. Turek, and S. Egginton, Concentric diffusion in tissue with heterogeneous permeability and consumption, in *Oxygen Transport to Tissue-XII*, Advances in Experimental Medicine and Biology, vol. 277, J. Piiper, T. K. Goldstick, and M. Meyer, eds., Plenum Press, New York and London, 1990, pp. 13–20.
11 L. Hoofd, Z. Turek, and J. Olders, Calculation of oxygen pressures and fluxes in a flat plane perpendicular to any capillary distribution, in *Oxygen Transport to Tissue-XI*, Advances in Experimental Medicine and Biology, vol. 248, K. Rakušan, G. P. Biro, T. K. Goldstick, and Z. Turek, eds., Plenum Press, New York and London, 1989, pp. 187–196.
12 L. Hoofd, J. Olders, and Z. Turek, A simple method to calculate oxygen fields in a tissue cross-section with arbitrary capillary distribution, in *Proc. 29th Dutch Fed. Mtg.*, Federation of Medical Scientific Societies, Nijmegen, The Netherlands, Abstract 175, 1988.
13 S. S. Kety, Determinants of tissue oxygen tension, *Fed. Proc.* 16:666–670 (1957).
14 F. Kreuzer, Oxygen supply to tissues: The Krogh model and its assumptions, *Experientia* 38:1415–1426 (1982).
15 F. Kreuzer and L. Hoofd, Facilitated diffusion of oxygen and carbon dioxide, in Handbook of Physiology: The Respiratory System: Gas Exchange, vol. IV, L. E. Fahri and S. M. Tenney, eds., American Physiological Society, Bethesda, Maryland, 1987, pp. 89–111.
16 A. Krogh, The number and distribution of capillaries in muscles with calculations of the oxygen pressure head necessary for supplying the tissue, *J. Physiol. London* 52:409–415 (1919).
17 R. F. Moran, J. L. Clausen, S. Ehrmeyer, M. Feil, A. L. Van Kessel, and J. H. Eichhorn, *Oxygen Content, Hemoglobin Oxygen, "Saturation," and Related Quantities in Blood: Terminology, Measurement, and Reporting*, NCCLS publication C25-P, vol. 10(2), Villanova, PA, 1990.
18 A. S. Popel, Analysis of capillary-tissue diffusion in multicapillary systems, *Math. Biosci.* 39:187–211 (1978).
19 A. S. Popel, Oxygen diffusive shunts under conditions of heterogeneous oxygen delivery, *J. Theor. Biol.* 96:533–541 (1982).

20 A. S. Popel, Theory of oxygen transport to tissue, *Crit. Rev. Biomed. Engrg.* 17:257–321 (1989).
21 J. S. Schultz, J. D. Goddard, and S. R. Suchdeo, Facilitated transport via carrier-mediated diffusion in membranes I. Mechanistic aspects, experimental systems and characteristic regimes, *AIChE J.* 20:417–445 (1974).
22 I. Sneddon, *Elements of Partial Differential Equations*, McGraw–Hill, New York, 1957.
23 P. Stroeve, Myoglobin-facilitated oxygen transport in heterogeneous red muscle tissue, *Ann. Biomed. Engrg.* 10:49–70 (1982).
24 Z. Turek, L. Hoofd, and K. Rakušan, Myocardial capillaries and tissue oxygenation, *Canad. J. Cardiol.* 2:98–103 (1986).
25 Z. Turek, K. Rakusan, J. Olders, L. Hoofd, and F. Kreuzer, Computed myocardial pO_2 histograms: Effects of various geometrical and functional conditions, *J. Appl. Physiol.* 70:1845–1853 (1991).